Separation and Purification Technology 332 (2024) 125828

Contents lists available at ScienceDirect

Separation and Purification Technology

journal homepage: www.elsevier.com/locate/seppur

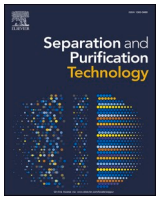

Optimal design of a simulated-moving-bed separation process for economical production of xylitol from bamboo-hydrolysis byproducts

Cheol Yeon Jo [a], Hyun Kyung Mo [a], Ki Bong Lee [b,*], Sungyong Mun [a,*]

[a] Department of Chemical Engineering, Hanyang University, 222, Wangsimni-ro, Seongdong-gu, Seoul, 04763, Republic of Korea
[b] Department of Chemical and Biological Engineering, Korea University, 145 Anam-ro, Seongbuk-gu, Seoul, 02841, Republic of Korea

ARTICLE INFO

Editor: Raquel Aires Barros

Keywords:
Simulated moving bed
Xylitol
Standing wave design
Process optimization
Continuous separation process

ABSTRACT

Xylitol, which is one of industrially useful sugar-alcohols, has received constant attention from various industries. For the eco-friendly and economical production of xylitol, the byproducts from bamboo hydrolysis treatments for bioethanol-production purposes can be utilized as the source for xylitol. Since such bamboo-hydrolysis byproducts were reported to consist of several polyols such as xylitol, xylose, and glycerol, one essential requirement for ensuring a large-scale production of xylitol will be to secure a highly-efficient process for separation of xylitol from the above-mentioned polyol mixture. To address this issue, we aimed to establish an optimal simulated-moving-bed (SMB) process that can accomplish the xylitol-separation task of interest in a continuous mode while maintaining the best performances. It was found first that the use of an ion-exchange resin of styrene–divinylbenzene copolymer in lanthanum form at 60 °C was most suitable as the adsorbent conditions of the xylitol-separation SMB. Under such adsorbent conditions, the intrinsic parameters of the polyol mixture components were determined and then applied to the optimization of the xylitol-separation SMB with a standard type of configuration (2–2–2–2), which was carried out based on the standing wave design method. It was confirmed that the optimized process was successful in keeping the front and rear of each solute band within their corresponding zones under the maximized degree of adsorbent utilization, which suggested that the yield of xylitol and the removal rates of non-products could be maintained at sufficiently high levels while maximizing the SMB throughput. Further comprehensive optimizations revealed that compared to the standard configuration-based SMB, the 5–2–7–2 configuration-based SMB can more than double the xylitol product concentration as well as almost halve the desorbent usage, while maintaining the same throughput and separation capability.

1. Introduction

There are several sugar-alcohols that have been found to be useful from an industrial point of view. Among them, it is worth paying particular attention to a five-carbon sugar-alcohol, xylitol, which is known to be effective in preventing dental caries, acute otitis, and cystic fibrosis, and also in serving as prebiotics as well as a sweetener for diabetics [1,2]. Due to such health benefits and medical efficacy, xylitol has received constant attention from food, health functional food, and pharmaceutical industries.

It was reported that the above-mentioned xylitol could be obtained through several pathways, of which the following two are noteworthy. The first pathway is to produce xylitol through catalytic hydrogenation of xylose [3,4], while the second pathway is to recover xylitol from the byproducts that can be caused by bamboo hydrolysis treatments for bioethanol-production purposes [2]. Between these two, it is particularly worth noticing the second pathway, because it deals with only the separation of xylitol from the bamboo-hydrolysis byproducts without involving a chemical reaction as in the first pathway. It is thus expected that the second pathway could be a more eco-friendly and economical xylitol-production mode.

According to the most recent literature [2], the bamboo-hydrolysis byproducts of the second pathway mentioned above consisted of several polyols such as xylitol, xylose, and glycerol. This suggests the need to establish an efficient process for separation of xylitol from such polyol mixture while ensuring high levels of separation capability and economical efficiency. To address this point, the aforementioned xylitol-separation process, which is targeted in this study, needs to be

* Corresponding authors.
E-mail addresses: kibonglee@korea.ac.kr (K.B. Lee), munsy@hanyang.ac.kr (S. Mun).

https://doi.org/10.1016/j.seppur.2023.125828
Received 18 October 2023; Received in revised form 16 November 2023; Accepted 21 November 2023
Available online 24 November 2023

developed based on an appropriate process mode that can enable both continuous injection of feed mixture and continuous collection of xylitol product stream while maintaining high levels of purity, yield, and throughput, and further reducing desorbent usage. One of such process modes with proven performances is a simulated-moving-bed (SMB), which has been in the limelight in many high-value industries to date [5–8].

Fig. 1 shows the operation mode and structure of an SMB process for binary separation. As seen in Fig. 1, an SMB consists of a number of columns filled with pre-selected adsorbent particles (solid phase), which are usually divided into four zones depending on the locations of four ports responsible for feed, desorbent, extract, and raffinate streams. The four ports are set to move by the length of one column along the liquid-phase flow direction at each specified time, which has been referred to as switching time [7]. If its design, as well as the design of zone flow rates, is carried out in a systematic way, it is possible to enable two outlet ports to be always located in partially separated regions of two solute bands while keeping a feed port placed in their mixed region. This state can allow an SMB process to implement a continuous-mode operation while ensuring that both the recovery of a product component and the removal of impurities can be fulfilled at an almost complete level, i.e. the yields of all components can be kept high. Due to these merits, an SMB can significantly outperform conventional batch chromatographic processes in all respects [6,9].

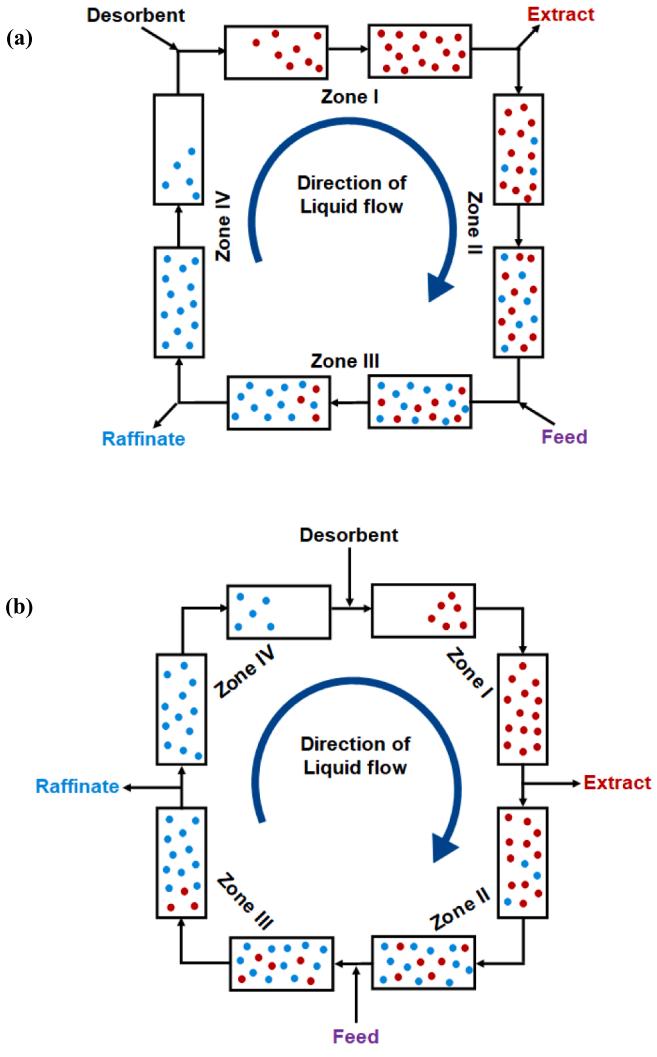

Fig. 1. Schematic diagram of a four-zone SMB process with a standard type of column configuration (2–2–2–2). (a) N^{th} step, (b) $(N + 1)^{th}$ step. ● : lower adsorption-affinity component (or fast-migrating component), ● : higher adsorption-affinity component (or slow-migrating component).

The goal of this study is to apply such SMB process mode to the separation of xylitol from the above-mentioned polyol mixture (corresponding to bamboo-hydrolysis byproducts) and further to establish the optimal xylitol-separation SMB process that can ensure the highest throughput and the lowest desorbent usage while maintaining high yields for all mixture components and also reducing the degree of product dilution. As the first step towards this task, the intrinsic parameters of the polyol mixture components (xylitol, xylose, and glycerol) on a commercially available ion-exchange resin (Amberchrom-50WX8 resin) were determined under properly selected resin ionic form and column temperature. The intrinsic parameters determined were utilized as the input parameters for promoting the optimal design of the xylitol-separation SMB process (abbreviated as "xylitol-SMB" from now on). To facilitate this task, the xylitol-SMB optimization tool was constructed based on the standing wave design (SWD) method [9,10], which has been proven accurate in performing SMB optimization through many previous studies and has also been acknowledged to have a clear advantage in extending the scope of SMB optimization targets [11,12]. Using the constructed SWD optimization tool, the xylitol-SMB process of interest was optimized, and then it was verified for separation performances and adsorbent utilization (indicative of throughput) through dynamic column profiles at a cyclic steady state. Finally, the optimal column configuration leading to a further improvement in xylitol product concentration without a reduction in separation performances and throughput was explored through a series of additional xylitol-SMB optimization runs.

2. Theory

2.1. Standing wave design (SWD) method for a linear isotherm SMB process with binary or pseudo-binary separation purpose

One of the important tasks in the stage of SMB design is the optimal determination of SMB operation parameters. This subject has been studied extensively and the related methods have been reported in previous researches. Among them, the SWD method has been recognized to provide an excellent level of computational efficiency while maintaining accuracy at a reasonable level, particularly for non-equilibrium systems with mass-transfer resistances to be considered [9–12]. The advantage of the SWD method over the triangle-theory method is that the SWD method reflects the effects of dispersion and mass-transfer resistance, which makes more accurate design possible [9].

The nub of the SWD method is to optimize the SMB operation parameters in a way that four key concentration waves can be forced to be trapped within their corresponding zones while maximizing the adsorbent utilization of each zone and minimizing the required amount of desorbent. Such concentration-wave conditions have been referred to as "standing-wave conditions" in the literature [10], and the identities of concentration waves to be made standing in each zone for a binary-separation SMB process in accordance with the SWD principle are specified in Fig. 2.

In an effort to establish the efficient way of obtaining the SMB operation parameters that can create the aforementioned standing-wave conditions, the relevant SWD equations were derived and their validity was verified theoretically and experimentally in previous studies [9,10]. The mathematical expressions of such SWD equations for a linear isotherm SMB with binary separation purpose (Fig. 2) are given below.

$$Q^I = S\left[\varepsilon_b + (1-\varepsilon_b)H_B\right]\nu + \frac{\varepsilon_b S \beta_B^I}{N_c^I L_c}\left[E_{b,B}^I + \frac{P(H_B\nu)^2}{K_{f,B}^I}\right] \equiv SWD(I,\ B) \tag{1a}$$

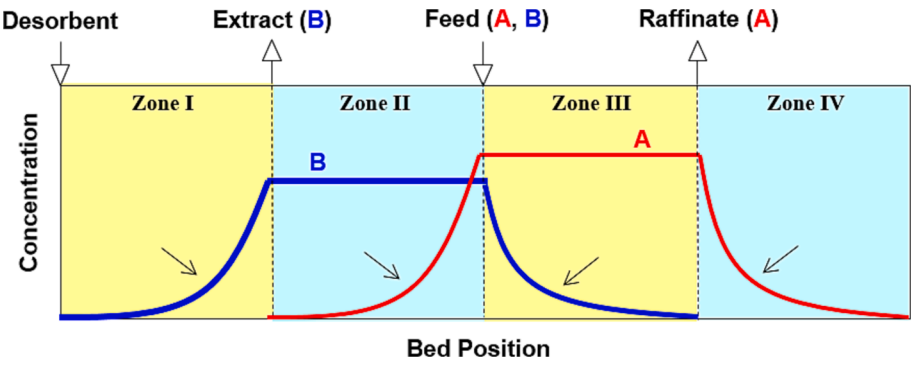

Fig. 2. Illustration of the standing-wave conditions in a linear-isotherm SMB process with binary separation purpose. A: lower adsorption-affinity component (or fast-migrating component), B: higher adsorption-affinity component (or slow-migrating component).

$$Q^{II} = S\left[\varepsilon_b + (1-\varepsilon_b)\,H_A\right]\nu + \frac{\varepsilon_b\, S\,\beta_A^{II}}{N_c^{II}\,L_c}\left[E_{b,A}^{II} + \frac{P\,(H_A\,\nu)^2}{K_{f,A}^{II}}\right] \equiv SWD\,(II\,,\ A) \tag{1b}$$

$$Q^{III} = S\left[\varepsilon_b + (1-\varepsilon_b)\,H_B\right]\nu - \frac{\varepsilon_b\, S\,\beta_B^{III}}{N_c^{III}\,L_c}\left[E_{b,B}^{III} + \frac{P\,(H_B\,\nu)^2}{K_{f,B}^{III}}\right] \equiv SWD\,(III\,,\ B) \tag{1c}$$

$$Q^{IV} = S\left[\varepsilon_b + (1-\varepsilon_b)\,H_A\right]\nu - \frac{\varepsilon_b\, S\,\beta_A^{IV}}{N_c^{IV}\,L_c}\left[E_{b,A}^{IV} + \frac{P\,(H_A\,\nu)^2}{K_{f,A}^{IV}}\right] \equiv SWD\,(IV\,,\ A) \tag{1d}$$

where the superscripts I to IV indicate zone number; the subscripts A and B stand for a lower adsorption-affinity (or fast-migrating) component and a higher adsorption-affinity (or slow-migrating) component respectively; Q^j is the volumetric flow rate in zone j; L_c is the column length; ν is the average port velocity (=column length / switching time); H is the linear adsorption parameter based on a particle-volume basis; E_b and K_f are the axial dispersion coefficient and lumped mass-transfer coefficient respectively; and the meanings of the other symbols in the above equations are presented in Supplementary Material. In the initial stages of SMB design, the feed flow rate (Q^{feed}) is usually preset (i.e., the Q^{feed} value is given in advance). Since Q^{feed} comes from the difference between Q^{II} and Q^{III}, the following relationship must be included in the SWD equation set above.

$$Q^{feed} = Q^{III} - Q^{II} \tag{1e}$$

Now, we have five equations (Eqs. (1a) to (1e)) for five unknowns (Q^I, Q^{II}, Q^{III}, Q^{IV}, and ν), indicating that closed-form solutions can be found. However, it is necessary to mention that E_b and K_f depend on the flow rate. This implies that it is not straightforward to solve Eqs. (1a) to (1e) for the targeted operation parameters (Q^I, Q^{II}, Q^{III}, Q^{IV}, and ν). It is thus necessary to perform repetitive calculations based on the method of trial and error in the following manner. First, the SWD equations omitting the terms containing E_b and K_f on the right sides of Eq. (1), i.e. the SWD equations under an equilibrium state are solved for the operation parameters of the 1st set, which virtually correspond to the initial guesses for Q^I, Q^{II}, Q^{III}, Q^{IV}, and ν. Based on the resulting zone flow rates (Q^j), one can calculate E_b and K_f, which are then used to solve the SWD equations containing all terms for the operation parameters of the 2nd set. The aforementioned execution is repeated until there is almost no difference between the previous set and the next set of operation parameters. Once the final set of operation parameters is determined, the switching time (t_{sw}) can be obtained simply from the following calculation; $t_{sw} = L_c/\nu$. It was reported that if the operation parameters resulting from the calculation of the above SWD equations were applied to the relevant SMB process, the maximum possible levels of adsorbent and desorbent utilization could be maintained while meeting most of the target yields for all components [10].

The coverage of the above SWD equations can also be extended to the design of a multi-component SMB process for a pseudo-binary separation task [10], under the premise that the identities of concentration waves to be made standing in each zone is changed in the manner described in Fig. 3. In the case of the pseudo-binary separation task under consideration in this study, xylitol (target product) corresponds to the highest adsorption-affinity component, while glycerol and xylose correspond to the intermediate-affinity and the lowest-affinity components respectively. Accordingly, the SWD equations applicable to the xylitol-SMB process of interest can be expressed as follows.

$$Q^{I} = SWD\,(I\,,\ \text{xylitol}) \tag{2a}$$

$$Q^{II} = SWD\,(II\,,\ \text{glucose}) \tag{2b}$$

$$Q^{III} = SWD\,(III\,,\ \text{xylitol}) \tag{2c}$$

$$Q^{IV} = SWD\,(IV\,,\ \text{xylose}) \tag{2d}$$

where the mathematical representations of the "*SWD*" operators can be found in Eq. (1). The computer program for automatic calculation of the above SWD equations (Eq. (2)) was constructed using FORTRAN, and then used as a tool for optimizing the operation parameters of the targeted xylitol-SMB process.

2.2. Column model for simulations

One of the effective ways for verifying the validity of SMB design results is to check whether the migration patterns of solute bands can be well aligned with the goal of SMB design. This task is usually facilitated by examining the cyclic-steady-state column profiles of the designed SMB, which can be obtained from simulations based on a proven column model. One of the widely used column models for such purpose is a lumped mass-transfer model, which has been recognized as being at a high level of both accuracy and applicability [9,10,13]. This model consists of a series of partial differential equations that can account for the phenomena of convection, dispersion, film mass-transfer, adsorption, and intra-particle diffusion occurring in an inter-particle liquid space, a solid surface, and an intra-particle liquid space (or pore). The relevant model equations for each column in SMB are given below [9,14].

$$\varepsilon_b\frac{\partial C_{b,i}}{\partial t} + (1-\varepsilon_b)\,K_{f,i}\,(C_{b,i} - C_i^*) + u_0\,\varepsilon_b\frac{\partial C_{b,i}}{\partial z} - \varepsilon_b\,E_{b,i}\,\frac{\partial^2 C_{b,i}}{\partial z^2} = 0 \tag{3a}$$

$$\frac{\partial q_i^*}{\partial t} = K_{f,i}(C_{b,i} - C_i^*) \tag{3b}$$

$$q_i^* = H_i\,C_i^* \tag{3c}$$

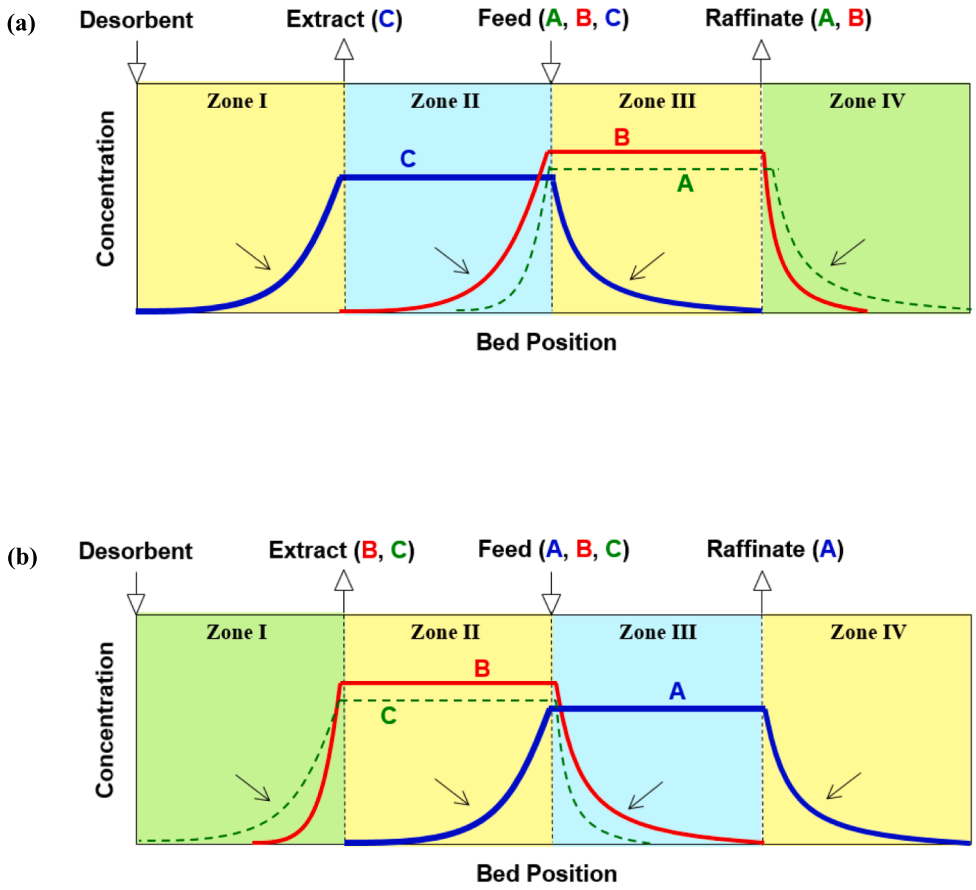

Fig. 3. Illustration of the standing-wave conditions in a linear-isotherm SMB process with pseudo-binary separation purpose. A: lowest adsorption-affinity component, B: Intermediate adsorption-affinity component, C: highest adsorption-affinity component. (a) SMB with component C as a target product, (b) SMB with component A as a target product.

where C and q stand for liquid and solid phase concentrations respectively; the subscript b means bulk space or inter-particle liquid space; the superscript * means pore space (for C) or equilibrium state (for q); and H_i is the linear adsorption parameter based on a particle-volume basis. The lumped mass-transfer coefficient (K_f) is a function of intra-particle diffusivity (D_p) and film mass-transfer coefficient (k_f) [10,11]. The relevant equation that connects K_f to D_p and k_f is presented in Supplementary Material. The tasks associated with solving the above model equations for column profiles (internal concentration profiles), which are usually referred to as simulation activities, were handled by Aspen Chromatography simulator.

3. Materials and methods

3.1. Materials

Xylitol, xylose, glycerol, and lanthanum (III) chloride hydrate were supplied from Sigma-Aldrich Co., and among them, the first three were used in determining the intrinsic parameters for the SMB design, while the last one was utilized in the resin pretreatment step for ionic-form conversion purpose. Distilled deionized water (DDW) and sulfuric acid aqueous solution were obtained from a Milli-Q system (Millipore Co.) and Yakuri Pure Chemicals Ltd. respectively. The former was used as a desorbent in the single-column experiments performed, and the latter was utilized in the preparation of a mobile-phase solution for HPLC concentration analysis.

Three types of Amberchrom-50WX series resins were purchased from Sigma-Aldrich Co., and used in the adsorbent screening stage for the separation work of interest. The ionic form of the finally selected resin (Amberchrom-50WX8) was converted from its original one (H^+) to a target one (La^{3+}) by following the reported procedure [2]. The Amberchrom-50WX8 adsorbent in La^{3+} form was filled in a glass column (1.5 × 22 cm) of Bio-Chem Fluidics Co. The average particle size of the adsorbent was 112 μm, and the inter-particle and intra-particle porosities of the filled column were 0.371 and 0.625 respectively, which were obtained from the relevant tracer-molecule pulse test and the literature [13] respectively.

3.2. Long-pulse injection experiments

For the purpose of identifying the adsorption and mass-transfer parameters of the SMB feed-mixture components, a series of single-column experiments based on a long-pulse injection mode were carried out at 60 °C by using a Young-Lin HPLC system. Before each of these experiments were started, a single column (1.5 × 22 cm) filled with the adopted adsorbent (Amberchrom-50WX8 resin in lanthanum form) was installed in the system, followed by pumping DDW into the column for pre-preparation. The experiment began by switching the pump flow from DDW to the feed solution containing each of the considered mixture components. The volume of the feed solution injected into the column was set relatively large so that the maximum level of solute concentration inside the column could reach a level close to the concentration of the feed solution, which actually corresponds to a general pattern of concentration profiles formed within SMB processes. Accordingly, the volume of the feed solution injected in the long-pulse injection experiment of this study was set at 40 mL for xylitol, 12 mL for glycerol, and 6 mL for xylose. Immediately after such feed injection was completed, DDW was eluted through the column. All of the

experiments described above were repeatedly performed under two different feed concentrations, one of which was chosen at the same level as the SMB feed concentration (10 g/L for each component) and the other at a lower level (6 g/L for each component). Throughout the experiments, the flow rate was maintained at 2 mL/min for both the feed injection and the DDW elution stages, and the data for the concentrations of the column effluent with respect to time was obtained with the help of a refractive index detector (Young-Lin 750F).

4. Results and discussion

4.1. Selection of adsorbent and column temperature

As far as the chromatographic separations of sugars and sugar-alcohols are concerned, it is widely known that ion-exchange resins of styrene–divinylbenzene copolymer series have high potential as an effective adsorbent. Accordingly, we first investigated the suitability of Amberchrom-50WX series resins, which are representative of the aforementioned type of ion-exchange resins. This task was conducted through preliminary pulse tests under three related resins (50WX2, 50WX4, and 50WX8 resins in H^+ form), which differ in the percentage of

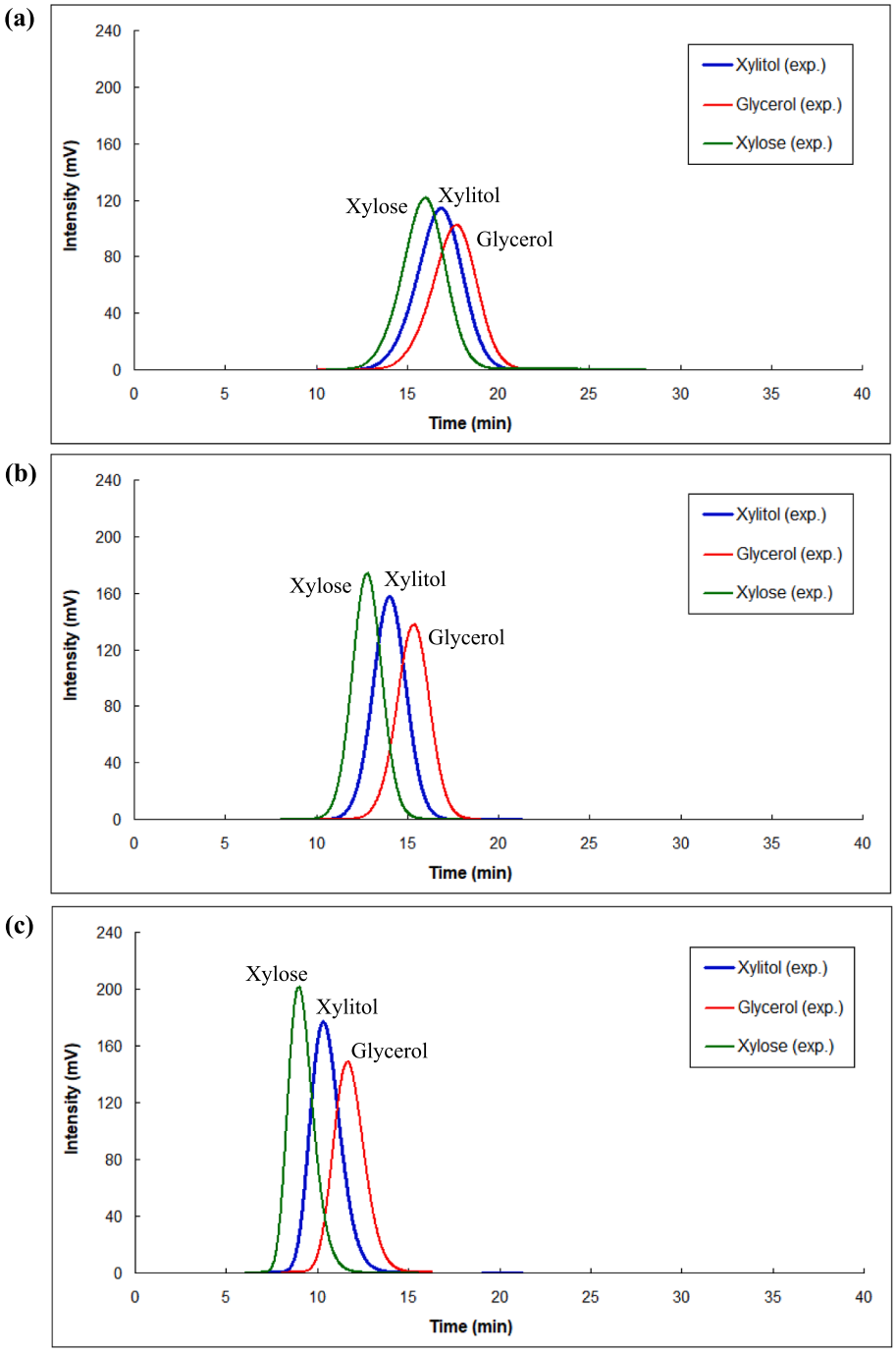

Fig. 4. Results of the preliminary pulse tests for screening a suitable adsorbent for xylitol separation among Amberchrom-50WX series resins. (a) 50WX2 resin (H^+), (b) 50WX4 resin (H^+), (c) 50WX8 resin (H^+). Column dimension: 1.5 × 22 cm, flow rate: 2 mL/min, injection volume: 500 μL, temperature: room temperature.

divinylbenzene in the resin copolymer (indicating the degree of resin crosslinkage). It was found that all the three tested resins did not offer a satisfactory level of xylitol separation capability (Fig. 4), and among them, the Amberchrom-50WX8 resin showed a little better separation potential than the other resins (Table 1). It is also necessary to notice in Fig. 4 that the elution order of xylitol is between those of xylose and glucose. This means that the recovery of xylitol from the considered mixture under the aforementioned resin will virtually correspond to a kind of ternary-separation task, which is usually known to require more processing time or more complex processing devices than binary or pseudo-binary separation tasks.

To make a further improvement in the xylitol-separation capability of the Amberchom-50WX8 resin, its ionic form was converted from its original form (H^+) to La^{3+} by referring to the relevant information in the literature [2]. From the results of the pulse tests using the Amberchom-50WX8 resin in La^{3+} form (shown in Fig. 5), it was confirmed that the aforementioned method of resin ionic-form conversion could lead to a significant improvement in the xylitol-separation capability. More importantly, xylitol was eluted last, not in the middle as before. This indicates that the xylitol-recovery task of our interest, if performed under the La^{3+}-loaded resin, can be treated like a kind of pseudo-binary separation task, which is certainly easier than ternary-separation tasks. In consideration of all the points mentioned above, the Amberchom-50WX8 resin in La^{3+} form was chosen as the adsorbent of the targeted SMB process in this study.

To determine the appropriate operating temperature of the column containing the above-selected adsorbent, a series of pulse tests were carried out while varying temperature. The results of these tests are presented in Fig. 5. It is readily seen that the column temperature has a large effect on the chromatographic behavior of xylitol but little effect on those of xylose and glycerol. The lower the column temperature, the more severe the back spread of the xylitol band (i.e., the spread of the rear of the xylitol band). This cases the xylitol band to become more asymmetric as the column temperature decreases (Fig. 5). Since a large degree of back spreading of the most strongly adsorbed component (corresponding to xylitol) hinders an efficient adsorbent regeneration, the column temperature in this study was set at 60 °C, the highest one in the investigated range. It is worth mentioning further that at the highest temperature (60 °C), the xylitol band shows the best symmetry.

4.2. Determination of intrinsic parameters related to adsorption and mass-transfer effects

Under the adsorbent and temperature selected above, we pursued an investigation into the intrinsic parameters of the target product (xylitol) and non-product components (xylose and glycerol), which included their adsorption and mass-transfer parameters and would serve as input parameters in the subsequent SMB design stage. For this task, a series of long-pulse injection experiments were carried out for each component while varying its feed concentration. The results of these experiments are presented in Fig. 6. It should be noted first that the retention time of each component is hardly affected by feed concentration and its band shape is quite symmetric, which implies that all the three components under consideration practically follow a linear adsorption pattern. Using the retention times from the experimental chromatograms in Fig. 6 and the solute movement theory [15], the linear adsorption parameters based on a particle-volume basis were determined, and the resulting parameter values are listed in Table 2.

Table 1
Comparison of Amberchrom-50WX series resins in terms of the selectivities for xylitol–xylose and xylitol–glycerol.

	50WX2 (H^+ form)	50WX4 (H^+ form)	50WX8 (H^+ form)
Xylitol / Xylose	1.101	1.190	1.776
Xylitol / Glycerol	1.089	1.175	1.424

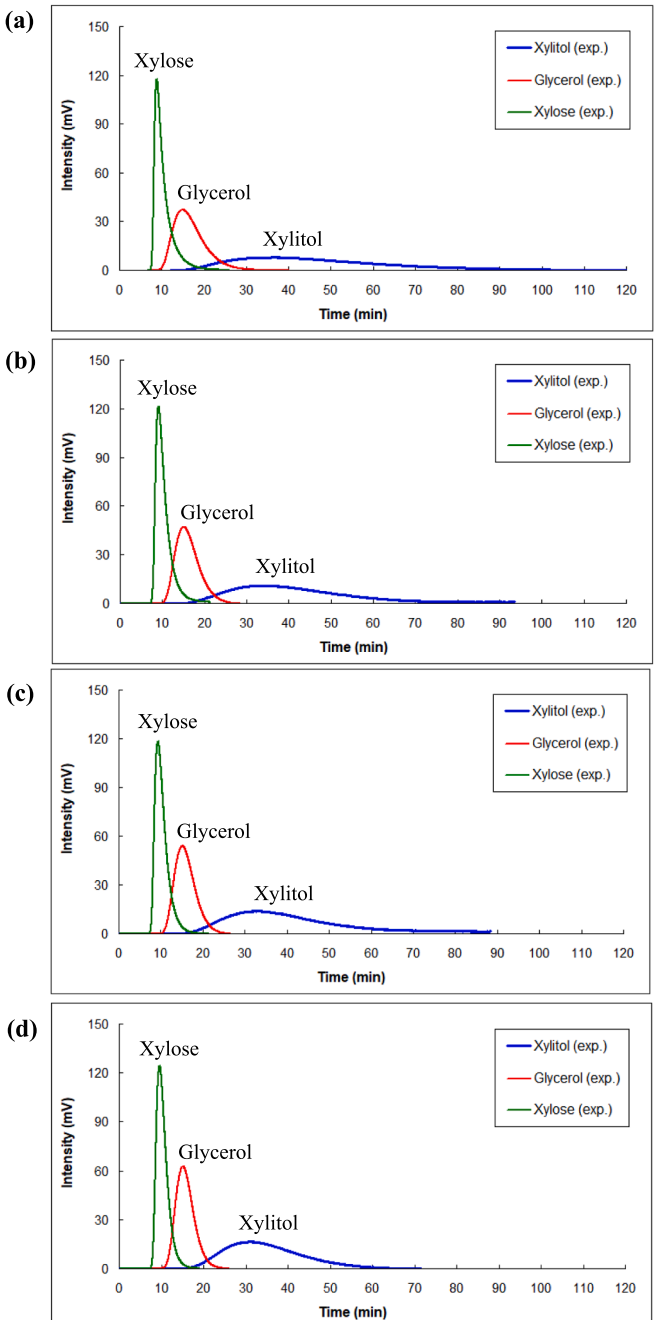

Fig. 5. Effect of temperature on the results of the pulse tests based on using the column packed with the Amberchrom-50WX8 resin in La^{3+} form. (a) Room temperature, (b) 40 °C, (c) 50 °C, (d) 60 °C. Column dimension: 1.5 × 22 cm, flow rate: 2 mL/min, injection volume: 500 μL.

In addition to the above-determined adsorption parameters, the mass-transfer parameters related to dispersion and mass-transfer resistance must be obtained for the SMB design. Regarding the acquisition of such mass-transfer parameters, those associated with molecular diffusion, dispersion, and film mass-transfer were estimated by using proven correlation equations [16–18], while the intra-particle diffusivity was determined by fitting the experimental data of Fig. 6 with the model-predicted profiles. The information on the sources for the applied correlation equations and the determined intra-particle diffusivity values are summarized in Table 2.

To check the validity of the intrinsic parameters that were estimated from literature correlation equations (Table 2), the column model based on these parameters was solved for column-effluent concentration

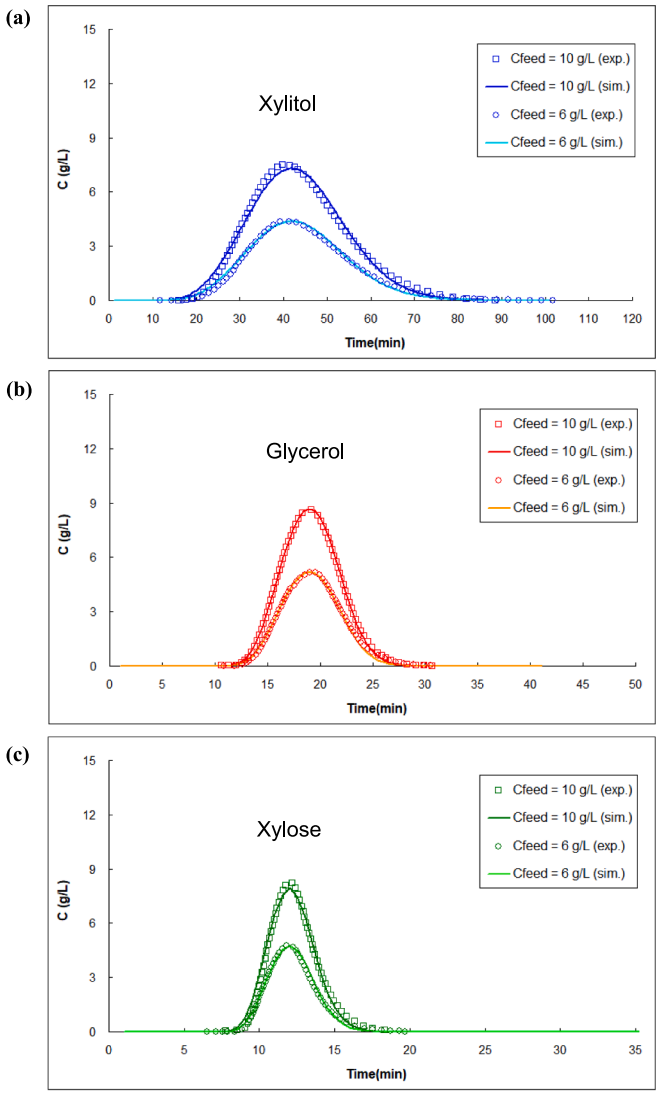

Fig. 6. Results of the long-pulse injection experiments based on using the column packed with the Amberchrom-50WX8 resin in La^{3+} form at 60 °C. (a) Xylitol (injection volume = 40 mL), (b) Glycerol (injection volume = 12 mL), (c) Xylose (injection volume = 6 mL). Column dimension: 1.5 × 22 cm, flow rate: 2 mL/min.

Table 2
Intrinsic parameters of the feed-mixture components to be treated by the targeted xylitol-SMB process based on using the Amberchrom-50WX8 resin (La^{3+} form) as an adsorbent under the temperature of 60 °C.

	Xylitol	Glycerol	Xylose
Linear adsorption parameter* (H)	2.065	0.647	0.200
Molecular diffusivity (D_∞), cm^2/min	4.61×10^{-3}	1.05×10^{-3}	1.13×10^{-3}
Intra-particle diffusivity (D_p), cm^2/min	2.00×10^{-6}	1.50×10^{-5}	1.30×10^{-5}
Axial dispersion coefficient (E_b), cm^2/min	Chung and Wen correlation [16]		
Film mass-transfer coefficient (k_f), cm/min	Wilson and Geankoplis correlation [17]		

* The linear adsorption parameters were based on a particle-volume basis.

histories under the conditions of the long-pulse injection experiments performed. The resulting concentration histories from the model prediction were then compared with the corresponding experimental data in Fig. 6, which demonstrates that the model-prediction results are closely aligned with the experimental data. It is therefore clear that the adopted correlation equations for intrinsic-parameter estimation (Table 2) have a level of accuracy sufficiently applicable to the optimal design of the targeted SMB process in this study.

4.3. Phase 1 of optimal design of the xylitol-SMB process

Using the intrinsic parameters determined above (Table 2), we pushed forward the optimal design of the xylitol-SMB process on the basis of the SWD method, in which the target yields of all components were set at 99.9 % under a column diameter of 3 cm and a feed concentration of 10 g/L (for each component). During the first design phase, the maximization of the xylitol-SMB throughput (i.e., feed flow rate) was pursued under a generally accepted column configuration, i.e. 2–2–2–2 (the mode of placing two columns evenly in each zone as in Fig. 1), while setting the length of each column at 30 cm. Based on these conditions, the SWD optimization for the xylitol-SMB, which was named "phase 1 optimization" in this study, was accomplished, and the resulting operation parameters are provided in the left side of Table 3.

To verify the validity of the above SWD design results, the column-model simulations were executed for the dynamic SMB column profiles under a cyclic steady state on the basis of the operation parameters in the left side of Table 3. The resultant column profiles in Fig. 7 show that the rear and front of xylitol band are well trapped within zones I and III respectively during the whole of each switching period at a cyclic steady state. At the same time, the rear of glycerol band and the front of xylose band are also well trapped within zones II and IV respectively. This also generates the additional effect of keeping the rear of xylose band and the front of glycerol band trapped within zones II and IV respectively, which is due to the fact that xylose is less strongly adsorbed than glycerol (Table 2). The results so far indicate that all the three components are mostly discharged through their corresponding outlet ports without contaminating the other outlet port, which will obviously ensure that the yields of all components can be very close to the target level (99.9 %).

Another notable point in Fig. 7 is that the migration ranges of the desorption wave (trailing wave) and adsorption wave (advancing wave) of xylitol band span the entire regions of zones I and III respectively. Similarly, the migration ranges of the glycerol desorption wave and the xylose adsorption wave also span the entire regions of zones II and IV respectively. These results suggest that the phase 1 optimized xylitol-SMB, which is listed in the left side of Table 3, can guarantee the highest level of adsorbent utilization and the lowest level of desorbent

Table 3
The results from the phase 1 and phase 2 optimizations for the xylitol-SMB process.

	Phase 1 SMB optimization	Phase 2 SMB optimization
Column configuration	2 – 2 – 2 – 2	5 – 2 – 7 – 2
Total number of columns	8	16
Single column length (cm)	30	15
Zone flow rates[a] and switching time: Q^j (mL/min), t_{sw} (min)	$Q^I = 12.7535$ $Q^{II} = 4.6378$ $Q^{III} = 7.3137$ $Q^{IV} = 2.9230$ $t_{sw} = 35.9267$	$Q^I = 6.7396$ $Q^{II} = 2.8129$ $Q^{III} = 5.4950$ $Q^{IV} = 1.7644$ $t_{sw} = 29.7028$
Inlet and outlet flow rates[b] (mL/min)	$Q^{feed} = 2.6759$ $Q^{des} = 9.8305$ $Q^{ext} = 8.1157$ $Q^{raf} = 4.3907$	$Q^{feed} = 2.6821$ $Q^{des} = 4.9752$ $Q^{ext} = 3.9267$ $Q^{raf} = 3.7306$
Ratio of xylitol product concentration to xylitol feed concentration ($C_{product}$ / C_{feed} for xylitol)	0.329	0.682
Desorbent usage (Q^{des} / Q^{feed})	3.674	1.855

[a] The superscripts of Q, i.e. I, II, III, and IV indicate zone number.
[b] The superscripts of Q, i.e. feed, des, ext, and raf indicate feed, desorbent, extract, and raffinate, respectively.

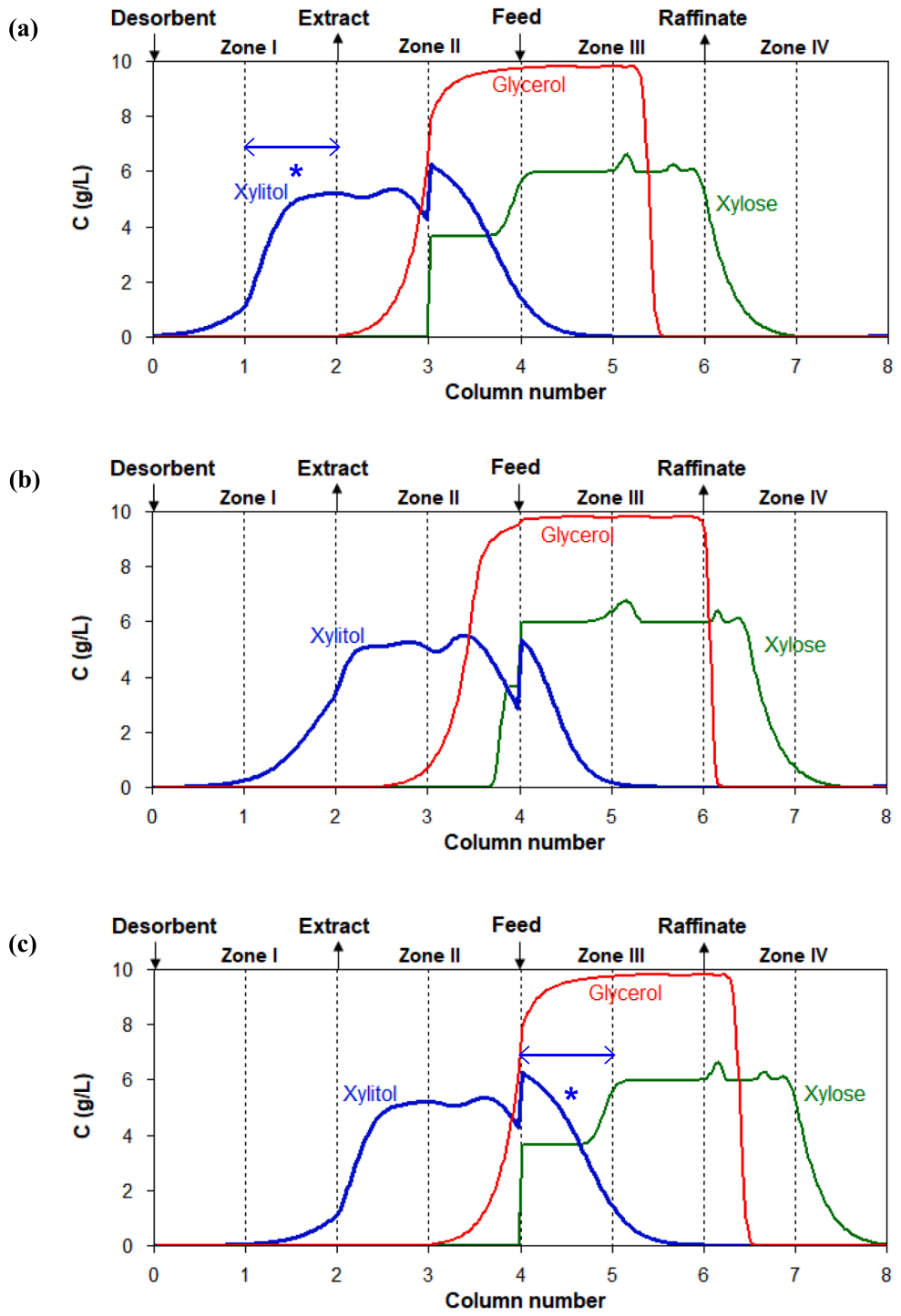

Fig. 7. Cyclic-steady-state column profiles of the optimized xylitol-SMB process (phase 1) based on the 2–2–2–2 configuration (refer to the left side of Table 3 for the SMB operating conditions). (a) Beginning of a cyclic-steady-state step, (b) Middle of a cyclic-steady-state step, (c) End of a cyclic-steady-state step.

usage.

4.4. Phase 2 of optimal design of the xylitol-SMB process

Although the above-optimized xylitol-SMB (phase 1) showed good performances in terms of separation capability and adsorbent utilization, it had serious problems of excessively low product concentration and excessively high desorbent usage, which can be identified in the lower left part of Table 3. This phenomenon is largely due to the fact that the adsorption strength and mass-transfer resistance of xylitol (product) are relatively very large, which can be recognized from the values of adsorption parameters and intra-particle diffusivities in Table 2.

To make a substantial improvement in xylitol product concentration and desorbent usage, it is worth considering the modification of the column configuration of the xylitol-SMB process. For this purpose, a series of SWD optimization runs for the xylitol-SMB process were conducted under different column configurations while keeping total column volume (i.e., total column length) and feed flow rate the same as those of the phase 1 optimized process based on the 2–2–2–2 configuration, namely, keeping throughput constant despite the change in the

column configuration. In these runs, if the total number of columns (TNC) increased while changing the column configuration, the single column length (L_c) of the xylitol-SMB was reduced accordingly in order to keep the total column length unchanged. The results from these optimization runs, which were named "phase 2 optimization" runs in this study, are presented in Fig. 8, where the ratio of xylitol product concentration to xylitol feed concentration ($C_{product}/C_{feed}$) and the desorbent usage (Q^{des}/Q^{feed}) are plotted as a function of TNC while marking the optimal column configuration at each TNC.

Note in Fig. 8a that the xylitol product concentration tends to increase as TNC increases. This is due to the fact that as TNC increases, the column configuration of the xylitol-SMB can be adjusted in a more favorable direction for improving the product concentration. Regarding this point, it is worth paying particular attention to the pattern of the column-configuration adjustment. It is seen in Fig. 8a that as TNC increases, more columns are placed in zones I and III where the rear and front of xylitol band are located respectively. This trend is consistent with the previous results in the literature [19], which reported that the increase of column numbers in the zones containing the two ends of a product solute band could be advantageous for reducing the extent of product dilution.

In particular, it is worth noting in Fig. 8a that, as a result of the above points, the xylitol product concentration of the phase 2 optimized process under the 5–2–7–2 configuration (TNC = 16 and L_c = 15 cm) can become more than twice as high as that of the phase 1 optimized process under the 2–2–2–2 configuration (TNC = 8 and L_c = 30 cm), although the two processes have the same total-column-volume and feed flow rate, i.e. the same throughput. To elucidate the reason for such phenomenon more clearly, the cyclic-steady-state column profiles of the 5–2–7–2 process was provided in Fig. 9, which can then be compared with those of the 2–2–2–2 process (Fig. 7). The first notable observation

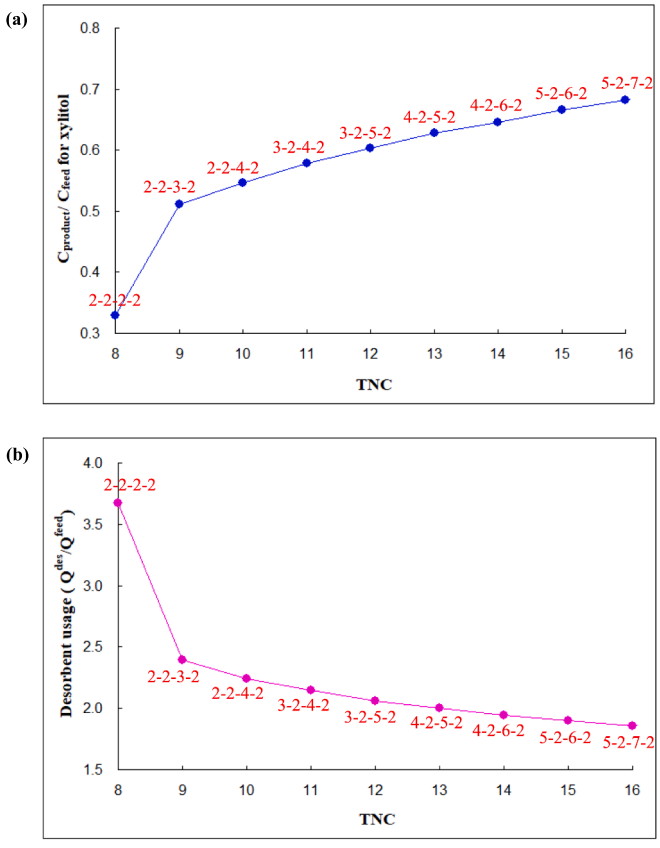

Fig. 8. Effect of column configuration on (a) the normalized xylitol product concentration and (b) the desorbent usage of the phase 2 optimized xylitol-SMB process according to TNC (total number of columns).

is that there is a definite difference in the level of xylitol concentration in the upstream column adjacent to an extract port, which is marked with an asterisk (Fig. 7a and 9a). It is readily seen that the level of xylitol concentration in the asterisked column is much higher in the 5–2–7–2 process than in the 2–2–2–2 process, which is obviously due to the fact that the increased number of columns in zone I (i.e., the upstream zone from the extract port) can help maintain a higher level of xylitol concentration in the zone I column directly in contact with the extract port. Similarly, it is worth noticing in Fig. 7c and 9c that the level of xylitol concentration in the downstream column adjacent to a feed port (marked by an asterisk) is much higher in the 5–2–7–2 process than in the 2–2–2–2 process, which is also due to the fact that the former has a larger number of columns in the downstream zone from the feed port than the latter. Since the aforementioned column will enter zone II (i.e., the zone containing the plateau region of xylitol band) after a subsequent port switching, the 5–2–7–2 process will be more advantageous in maintaining a higher level of xylitol plateau concentration in zone II, which will, in turn, help increase the xylitol product concentration through the extract port.

Due to the reasons mentioned above, the 5–2–7–2 process, i.e. the xylitol-SMB with more columns in the upstream zone from the extract port (zone I) and the downstream zone from the feed port (zone III) will be much more advantageous in terms of xylitol product concentration than the 2–2–2–2 process, i.e. the xylitol-SMB with the same number of columns in each zone. Since the attainment of higher product concentration indicates the occurrence of less dilution, the xylitol-SMB in favor of higher product concentration will ultimately have a lower degree of desorbent usage. As a result, the 5–2–7–2 process not only can more than double the xylitol product concentration (Fig. 8a), but also can reduce the desorbent usage by almost half (Fig. 8b), compared to the 2–2–2–2 process, while maintaining the same throughput and separation capability. It is thus concluded that the xylitol-SMB optimized under the 5–2–7–2 configuration in the right side of Table 3 can be one of the most suitable processes for continuous-mode recovery of xylitol from the polyol mixture corresponding to bamboo-hydrolysis byproducts.

5. Conclusions

This study proposed the optimal simulated-moving-bed (SMB) process for continuous-mode separation of xylitol from the polyol mixture that could be caused by bamboo hydrolysis treatments for bioethanol-production purposes. Regarding the adsorbent for such SMB process (named "xylitol-SMB"), the use of an Amberchrom-50WX8 resin in lanthanum form at 60 °C was found to be most appropriate in consideration of selectivity, the order of xylitol adsorption affinity, and the extent of xylitol band spread. Under such conditions of adsorbent and temperature, the intrinsic parameters related to adsorption and mass-transfer effects were investigated. The resulting intrinsic parameters were then used in the stage of optimizing the xylitol-SMB process with a standard type of column configuration (2–2–2–2), which was facilitated by using the SWD-based optimization tool. Such xylitol-SMB optimized under the 2–2–2–2 configuration was found to ensure a sufficiently high level of separation capability under the maximized degree of adsorbent utilization, which was verified through its dynamic column profiles. It was further revealed that the xylitol-SMB of 5–2–7–2 configuration can more than double the xylitol product concentration as well as almost halve the solvent usage, compared to the xylitol-SMB of 2–2–2–2 configuration, under the same throughput and separation capability.

CRediT authorship contribution statement

Cheol Yeon Jo: Methodology, Software, Validation, Formal analysis, Investigation, Visualization, Writing – original draft. **Hyun Kyung Mo:** Methodology, Validation, Investigation, Writing – original draft. **Ki Bong Lee:** Conceptualization, Methodology, Software, Writing – original draft, Writing – review & editing. **Sungyong Mun:**

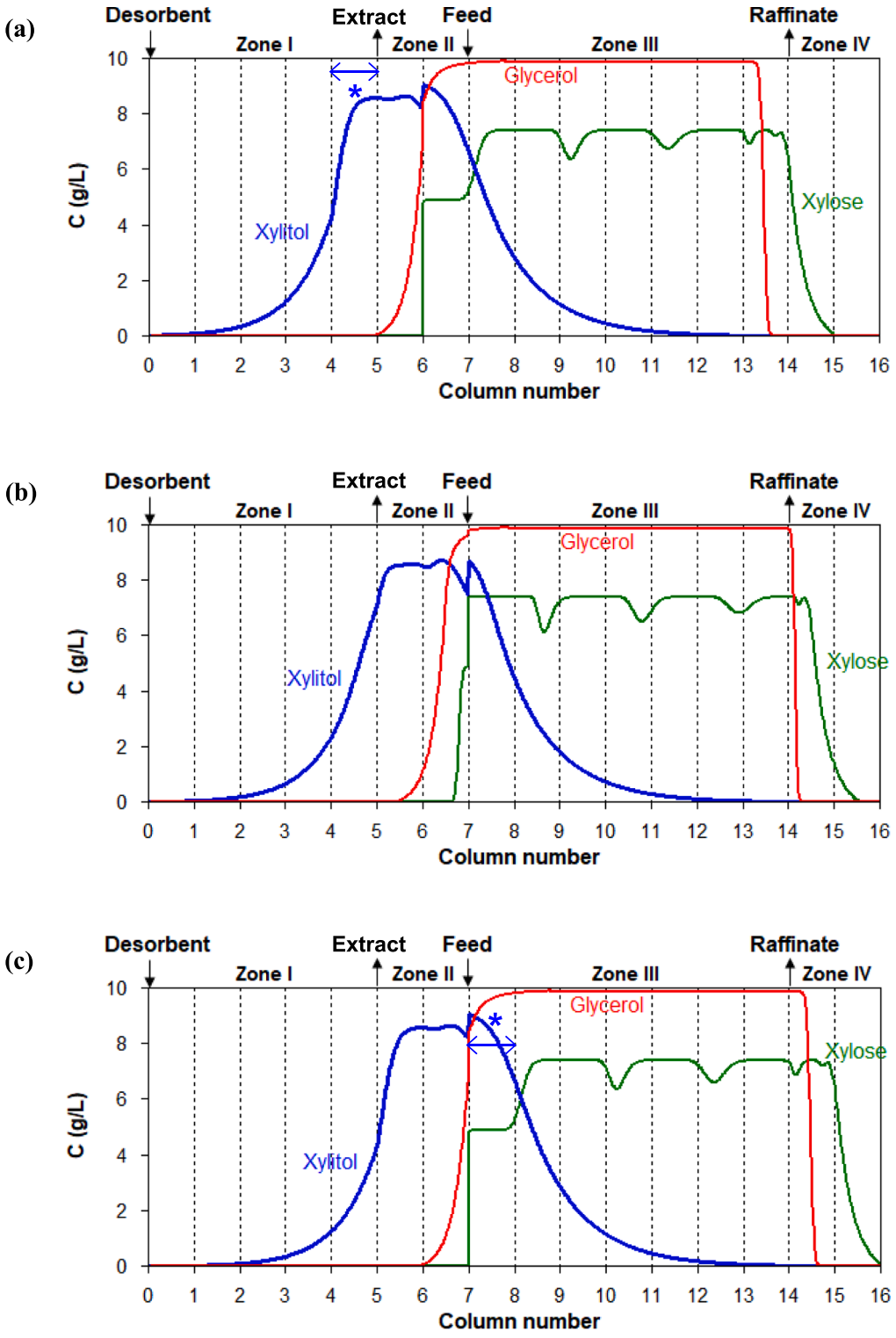

Fig. 9. Cyclic-steady-state column profiles of the optimized xylitol-SMB process (phase 2) based on the 5–2–7–2 configuration (refer to the right side of Table 3 for the SMB operating conditions). (a) Beginning of a cyclic-steady-state step, (b) Middle of a cyclic-steady-state step, (c) End of a cyclic-steady-state step.

Conceptualization, Methodology, Software, Writing – original draft, Writing – review & editing, Supervision, Project administration, Funding acquisition.

Declaration of competing interest

The authors declare that they have no known competing financial interests or personal relationships that could have appeared to influence the work reported in this paper.

Data availability

Data will be made available on request.

Acknowledgments

This research was supported by Basic Science Research Program through the National Research Foundation of Korea (NRF) funded by the Ministry of Science and ICT (grant number NRF-2023R1A2C2003115), and also by the Commercializations Promotion Agency for R&D Outcomes(COMPA) grant funded by the Korea government (MSIT) (No. 2023B210). This work was also partially supported by the Graduate school of Post Plastic specialization of Korea Environmental Industry & Technology Institute grant funded by the Ministry of Environment, Republic of Korea.

References

[1] D. Camargo, L. Sene, D.I.L.S. Variz, M.D.G.D. Almeida Felipe, Xylitol bioproduction in hemicellulosic hydrolysate obtained from sorghum forage biomass, Appl. Biochem. Biotechnol. 175 (2015) 3628–3642.
[2] Y. Kitamura, R. Shobu, H. Matsuura, A. Jyo, T. Ihara, Xylitol separation from a polyol mixture using lanthanide ion-loaded resins, Anal. Sci. 36 (2020) 769–773.
[3] M. Yadav, D.K. Mishra, J.S. Hwang, Catalytic hydrogenation of xylose to xylitol using ruthenium catalyst on NiO modified TiO2 support, Appl. Catal. A-Gen. 425 (2012) 110–116.
[4] N. Ullah, F. Jerome, K.D. Vigier, Hydrogenation of xylose to xylitol in the presence of bimetallic nanoparticles Ni_3Fe catalyst in the presence of choline chloride, Catalysts 12 (2022) 841.
[5] Y.S. Bae, C.H. Lee, Partial-discard strategy for obtaining high purity products using simulated moving bed chromatography, J. Chromatogr. A 1122 (2006) 161–173.
[6] J.S. Hur, P.C. Wankat, Chromatographic and SMB center-cut separations of ternary mixtures, Sep. Sci. Tech. 43 (2008) 1273–1295.
[7] P.S. Gomes, M. Zabkova, M. Zabka, M. Minceva, A.E. Rodrigues, Separation of chiral mixtures in real SMB units: The FlexSMB-LSRE (R), AIChE J. 56 (2010) 125–142.
[8] J.W. Lee, Expanding simulated moving bed chromatography into ternary separations in analogy to dividing wall column distillation, Ind. Eng. Chem. Res. 59 (2021) 9619–9628.
[9] Z. Ma, N.H.L. Wang, Standing wave analysis of SMB chromatography: Linear systems, AIChE J. 43 (1998) 2488–2508.
[10] B.J. Hritzko, Y. Xie, R. Wooley, N.H.L. Wang, Standing wave design of tandem SMB for linear multicomponent systems, AIChE J. 48 (2002) 2769–2787.
[11] K.B. Lee, C.Y. Chin, Y. Xie, G.B. Cox, N.H.L. Wang, Standing wave design of a simulated moving bed under a pressure limit for enantioseparation of phenylpropanolamine, Ind. Eng. Chem. Res. 44 (2005) 3249–3267.
[12] K.B. Lee, R.B. Kasat, G.B. Cox, N.H.L. Wang, Simulated moving bed multiobjective optimization using standing wave design and genetic algorithm, AIChE J. 54 (2008) 2852–2871.
[13] P.H. Kim, H.G. Nam, C. Park, N.H.L. Wang, Y.K. Chang, S. Mun, Simulated moving bed separation of agarose-hydrolyzate components for biofuel production from marine biomass, J. Chromatogr. A 1406 (2015) 231–243.
[14] H. Park, J.H. Choi, K.W. Bae, S. Mun, Continuous recovery of high-grade prebiotic ingredient from crude galacto-oligosaccharides using a simulated-moving-bed technology, J. Ind. Eng. Chem. 106 (2022) 362–373.
[15] P.C. Wankat, Rate-Controlled Separations, Blackie Academic & Professional, New York, 1994.
[16] S.F. Chung, C.Y. Wen, Longitudinal dispersion of liquid flowing through fixed and fluidized beds, AIChE J. 14 (1968) 857–866.
[17] E.J. Wilson, C.J. Geankoplis, Liquid mass transfer at very low Reynolds numbers in packed beds, Ind. Eng. Chem. Fundam. 5 (1966) 9–14.
[18] C.R. Wilke, P.I.N. Chang, Correlations of diffusion coefficients in dilute solutions, AIChE J. 1 (1955) 264–270.
[19] S. Mun, Consideration of a target product concentration level in the optimal design of a four-zone simulated moving bed process for binary separation, Chem. Eng. J. 204–206 (2012) 179–187.